

SO₂ Plumes Observation with LMOL: Theory, Modeling, and Validation

Guillaume Gronoff^{1,2}[0000-0002-0331-7076], Timothy Berkoff¹, William Carrion^{1,2}, Liqiao Lei^{1,2}[0000-0001-5833-8061], and Daniel Phoenix^{1,2}[0000-0003-2075-5374]

¹ NASA Langley Research Center, Hampton, Va, USA

Guillaume.P.Gronoff@nasa.gov

² Science Systems and Application Inc., Hampton, Va, USA

Abstract. LMOL, the NASA Langley Mobile Ozone Lidar, is located near NASA's LaRC steam plant when not deployed in campaigns. The plant produces steam through the incineration of local trash, and its exhaust plume occasionally contains SO₂.

SO₂ is a known, regulated, pollutant that affects O₃ observations in the UV, as is the case with LMOL. In this work, we show how we modified LMOL to detect the plant SO₂ plumes and compute its density when the O₃ background is stable; we observed densities compatible with what is expected from the typical plume exhaust. The selection of laser lines so that an O₃ variation would not get confused with a SO₂ detection is explained in details, and a model capable of simulating the Lidar signal with (notably) O₃ and SO₂ absorption for the validation of the retrieval resolution and uncertainty is presented. Finally, the comparison between the modeled and observed performances of the system is shown: the maximum altitude, resolution, and error in the modeled signal and the observed signals are the same within reasonable margins.

This work demonstrates that LMOL is fully capable of working with SO₂. The next step being the addition of an additional laser channel, which is simplified by the tunable aspect of the LMOL laser, to address O₃ and SO₂ simultaneously, allowing the assessment of SO₂ when O₃ has variations.

Keywords: Lidar · SO₂ · Ozone · Air Quality.

1 Introduction

1.1 LMOL

LMOL, the NASA Langley Mobile Ozone Lidar, [1], is a tunable dial lidar: it is currently able to shot at two wavelengths in the 285-292 nm range from a change in a software parameter (it is being developed for 4 wavelength operations). LMOL is part of the TOLNET network and has been used for several campaigns, notably dedicated to study the air quality [3, 5, 4]. Retrieving SO₂ with the lidar, in addition to O₃ would allow better understanding the local pollution sources.

1.2 The Hampton Steam Plant

The NASA / Hampton steam plant (<https://hampton.gov/2255/HamptonNASA-steam-plant>) is located North of NASA LaRC's location of LMOL (Figure 1). It converts the local trash into steam through incineration, the steam is used for local operations at NASA LaRC. The 2019 data gives an estimated yearly ejection of 10 tons of SO_2 after scrubbing by the different filtering systems. The stack, which rejects the exhaust at 75 m altitude high, is at a distance of 500 m from the location of LMOL from its 2019-2020 operations [4].

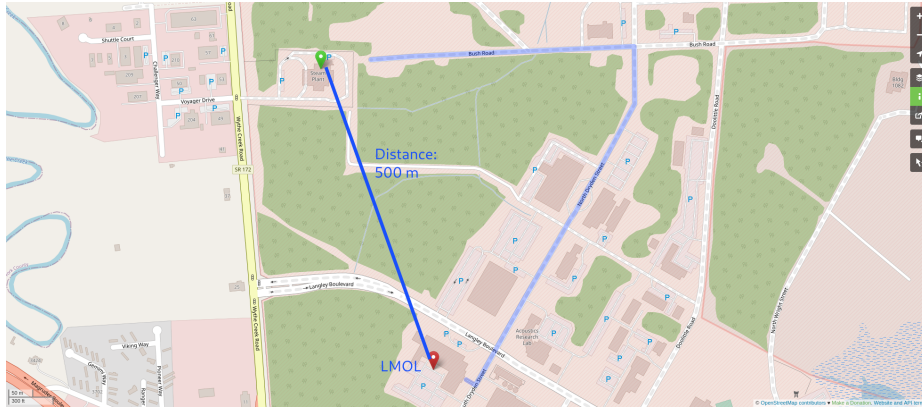


Fig. 1. The Hampton steam plant and its location relative to LMOL

2 Retrieval theory

In the following, we will describe how we use the DIAL procedure to retrieve SO_2 with our lidar and we explain the sensitivity approach.

In the DIAL procedure, the lidar signals -sent on two different wavelengths- are compared with each other; the differential absorption allows to retrieve the density of the absorbing species at each altitude bin. The highly absorbed wavelength is called the ONLINE, the less absorbed one is the OFFLINE. In the wavelength range available, SO_2 and O_3 are major absorbers. If one uses the 286 and 292 wavelength, SO_2 absorption is negligible compared to O_3 's, which means that the LMOL operations in O_3 are easy. In addition, the difference in absorption is high (around 10^{-18}cm^2), which means that the sensitivity of the lidar is high. If $P \cdot R^2$ is the returning power of the lidar in function of R , the range (and z the altitude), if we neglect the aerosol and the Rayleigh contribution, then we have the following equation

$$\Delta\sigma_{\text{SO}_2} N_{\text{SO}_2} + \Delta\sigma_{\text{O}_3} N_{\text{O}_3} = \frac{1}{2} \frac{\partial}{\partial z} \left[\ln \left(\frac{P_{\lambda_2}}{P_{\lambda_1}} \right) \right]$$

where $\Delta\sigma$ is the difference between the cross sections for the two wavelength. If the SO_2 density was negligible, then λ_2 would be the offline wavelength (see

Figure 2). For retrieving the SO₂ density with 2 wavelength from that equation, one should have stable O₃ background that could be subtracted and use a set of wavelengths optimized for the maximum SO₂ absorption (along with optimized laser power).

In the present study, we used the inverted wavelength technique: the ONLINE for SO₂ absorption would be the OFFLINE for the O₃ absorption and vice-versa. This means that if the change in absorption is due to more O₃, the algorithm would detect a negative change of SO₂. In the case of the observation of point sources of SO₂, as it is the case here, this means that the system would give a negative value of SO₂ density, showing that the hypothesis of stable O₃ background is not met. (Said simply, $\Delta\sigma_{SO_2}$ and $\Delta\sigma_{O_3}$ have opposite signs).

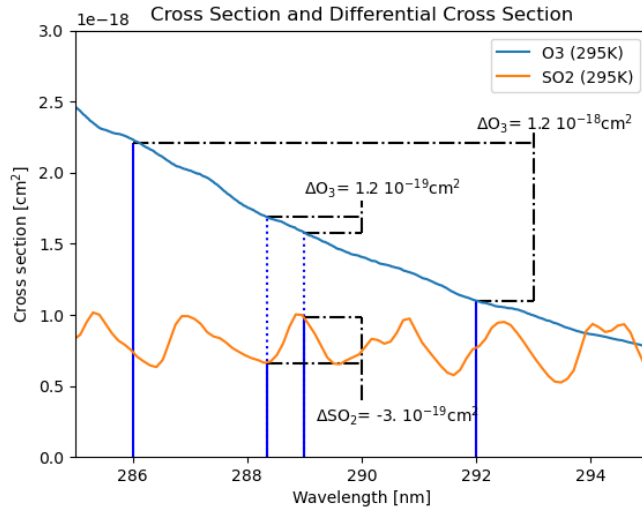


Fig. 2. The SO₂ and O₃ cross sections in the wavelength range available to LMOL. This figure shows how the wavelength are selected

The use of the 288.34 and 288.99nm wavelengths means that the change in O₃ density should be about -3 times the change in SO₂ density to get the same retrieved value (the system is more sensitive to SO₂). The small cross-section delta means that the sensitivity of SO₂ is smaller than the sensitivity in O₃ during the normal (286-292nm) operations. Therefore, validation of the sensitivity with simulations is necessary.

3 Simulation

We used the lidar simulation of LibRadtran [2] to compute the return of lidar for LMOL for its O₃ and SO₂ operations. LMOL is composed of two main telescopes:

the far field and the near field. These telescopes have different diameter and angular resolutions optimized for retrieving the data in the 100 m-2 km altitude for the near field and 1.5 km-10 km for the far field. Both of these channels were simulated with two wavelength, using different values of O_3 and SO_2 background to compare the theory with the actual observations. A first comparison of the model with the observations was made for the standard O_3 data: the 296 and 292 nm wavelength were simulated with a standard background of 100 PPBV of O_3 . This allowed to discover a loss of sensitivity of a PMT in 2019: the difference in sensitivity of the system between the far field and the very near field was not consistent with the difference in the mirror diameters. Once the PMT was changed, the theory and experiment matched. The addition of a solar background in the model allowed to match the retrieved upper altitude in both model and experiment when performing O_3 retrievals. At this point, it was possible to simulate the SO_2 data and try to validate its retrieval. In addition, we added an optional O_3 background to verify how it affected the retrieved SO_2 (if it is stable, it gives a negative bias in the results that can be later corrected). The results for the far field and very near field for the SO_2 simulations are displayed in Figure 4. It shows that the system can retrieve SO_2 with a correct vertical resolution for 5 minute averaging time. It is able to reach 2000m altitude for the dayside and 5000m in the nightside. Increasing the time averaging results in better vertical resolution (and higher maximum altitude in the nighttime; the dayside being limited by the solar background).

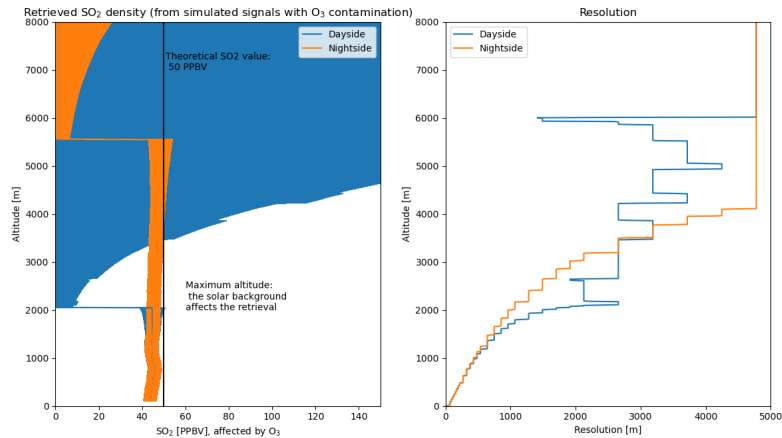


Fig. 3. Simulated retrieval of SO_2

4 Observation

LMOL typically performs observations of O₃ from NASA LaRC. The nighttime usually present very low values of O₃ at low altitude, of the order of 10/20 PPBV below 2000m, stable during the night. These values are however sometime affected by “strange” noise below 200m altitude. Using the 288 nm doublet optimized for SO₂ observations, we performed the retrieval of the night of 2020-02-18 to 2020-02-19. Around 03h UTC, the wind was blowing from the north at about 0.5 m/s, and values of the order of 80-100 PPBV on a vertical range of 50m at around 250 - 300m altitude. If we suppose that, at the location of LMOL, the plume of the power plant has a cross-section of 2500m² (i.e. a section of height/width near 50m) with a speed of 0.5m/s, then a 10 tons emissions per year gives a SO₂ density of 90 PPBV, which is what we observe. This very simple comparison shows that we are observing the order of magnitude expected for the plant plume. However, we do not have the spatial resolution to observe the whole cross section of the plume, nor do we know the variations in time of the emitted SO₂. Better models of the plume and comparison with realtime sensors at the plant may allow a better appreciation of the capabilities of the LMOL in its SO₂ configuration. Overall, the system is able to observe SO₂ in a meaningful way for performing work relevant to local air quality / the observation of point sources.

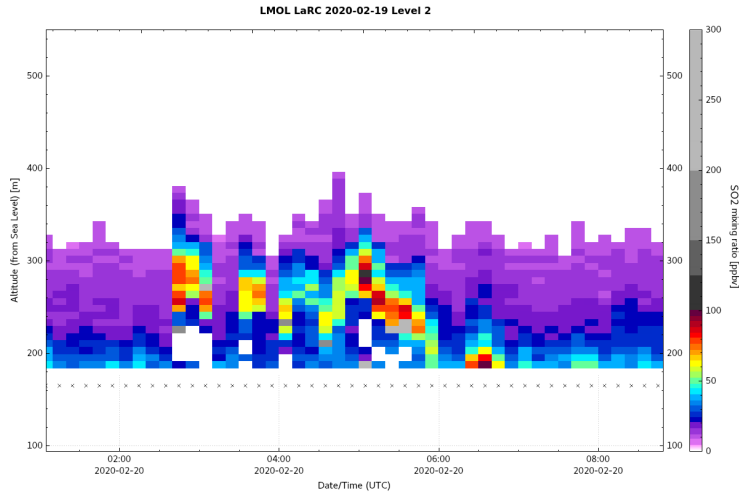


Fig. 4. Observed SO₂ plume from the Hampton Steam Plant

5 Future work

The current work shows that the use of two wavelength optimized for SO₂ retrieval allows LMOL to perform real-life observation of SO₂ plumes. The com-

parison of the observation with the expected values is excellent. However, these observations are limited by the O_3 background, which is expected to be stable for these observations. If one were to use 3 wavelength, this limitation could be lifted. The following set of equations could be solved provided the 3 wavelength are different (and the different determinant non-zero).

$$\Delta_1 \sigma_{SO_2} N_{SO_2} + \Delta_1 \sigma_{O_3} N_{O_3} = \frac{1}{2} \frac{\partial}{\partial z} \left[\ln \left(\frac{P_{\lambda_2}}{P_{\lambda_1}} \right) \right] \quad (1)$$

$$\Delta_2 \sigma_{SO_2} N_{SO_2} + \Delta_2 \sigma_{O_3} N_{O_3} = \frac{1}{2} \frac{\partial}{\partial z} \left[\ln \left(\frac{P_{\lambda_2}}{P_{\lambda_3}} \right) \right] \quad (2)$$

To optimize the sensitivity (and reduce the data processing noise) a set of 2 wavelength only sensitive to O_3 would allow to correct the O_3 background and the additional wavelength would maximize the sensitivity to SO_2 while minimizing the sensitivity to O_3 . A 4 channels system was purchased for performing these studies. The laser system is currently being modified to produce these 4 wavelengths.

Acknowledgements LMOL, part of the TOLNET project is funded by the NASA Tropospheric Composition Program, the Tropospheric Ozone Lidar network (TOLNET) and Langley Internal Research and Development program (IRAD) for the development of the SO_2 capabilities.

References

1. De Young, R., Carrion, W., Gano, R., Pliutau, D., Gronoff, G., Berkoff, T., Kuang, S.: Langley mobile ozone lidar: ozone and aerosol atmospheric profiling for air quality research. *Applied Optics* **56**(3), 721 (Jan 2017). <https://doi.org/10.1364/AO.56.000721>
2. Emde, C., Buras-Schnell, R., Kylling, A., Mayer, B., Gasteiger, J., Hamann, U., Kylling, J., Richter, B., Pause, C., Dowling, T., Bugliaro, L.: The libRadtran software package for radiative transfer calculations (version 2.0.1). *Geoscientific Model Development* **9**(5), 1647–1672 (May 2016). <https://doi.org/10.5194/gmd-9-1647-2016>
3. Farris, B.M., Gronoff, G.P., Carrion, W., Knepp, T., Pippin, M., Berkoff, T.A.: Demonstration of an off-axis parabolic receiver for near-range retrieval of lidar ozone profiles. *Atmospheric Measurement Techniques* **12**(1), 363–370 (Jan 2019). <https://doi.org/10.5194/amt-12-363-2019>
4. Gronoff, G., Berkoff, T., Knowland, K.E., Lei, L., Shook, M., Fabbri, B., Carrion, W., Langford, A.O.: Case study of stratospheric intrusion above Hampton, Virginia: Lidar-observation and modeling analysis. *Atmospheric Environment* **259**, 118498 (Aug 2021). <https://doi.org/10.1016/j.atmosenv.2021.118498>
5. Gronoff, G., Robinson, J., Berkoff, T., Swap, R., Farris, B., Schroeder, J., Halliday, H.S., Knepp, T., Spinei, E., Carrion, W., Adcock, E.E., Johns, Z., Allen, D., Pippin, M.: A method for quantifying near range point source induced O_3 titration events using Co-located Lidar and Pandora measurements. *Atmospheric Environment* **204**, 43–52 (May 2019). <https://doi.org/10.1016/j.atmosenv.2019.01.052>